Neurological Sciences (2019) 40:2333–2342
https://doi.org/10.1007/s10072-019-03981-6

ORIGINAL ARTICLE

Diffusion tensor imaging reveals abnormal brain networks in elderly subjects with subjective cognitive deficits

Daegyeom Kim[1] · Suji Lee[2] · Myungwon Choi[1] · HyunChul Youn[3] · Sangil Suh[4] · Hyun-Ghang Jeong[2,3] · Cheol E. Han[1]

Received: 13 February 2019 / Accepted: 13 June 2019 / Published online: 26 June 2019

Abstract

Purpose Some elders with subjective cognitive deficits (SCD) develop prodromal phase of dementia over time; however, little is known about how they differ from those with normal cognition (NC). Thus, we aim to distinguish the differences in the brain network of elders with SCD and NC.

Methods Multiple diffusion-weighted images (DWI) and T1-weighted images were obtained from 18 subjects with NC and 26 subjects with SCD. Using network-based statistics (NBS) analysis, we extracted abnormal brain subnetworks and localized abnormal brain connectivity. We also ran correlation analysis to compare the affected regions and the results of the neurocognitive assessments.

Results Altered subnetworks were found in the superior parietal gyrus, angular gyrus, precuneus, posterior cingulum, putamen, precentral gyrus, postcentral gyrus, and paracentral lobule. They were also associated with scores on the word list recall, word list recognition, and Boston naming test.

Conclusions Elders with SCD had distinctive brain network alterations when compared with those of elders with NC. The results are also in line with the previously identified characteristics of mild cognitive impairment (MCI) and of Alzheimer's disease (AD) in a milder form. We speculate that it may be possible to predict AD progression early in the SCD stage using NBS analysis.

Keywords Subjective cognitive deficits · Network-based statistics · Mild cognitive impairment · Alzheimer's disease · Cognitive function

Introduction

Subjective cognitive deficits (SCD) refer to cognitive dysfunction that individuals experience without any pathological indication on neurocognitive assessment results [1]. Often times, elderly adults with dementia syndromes undergo the phase of SCD before the onset of the disease [2–4]. Although there are emerging interests and accumulating evidence supporting an association between SCD and its progression to mild cognitive impairment (MCI) and Alzheimer's disease (AD), the opinions on classification and significance of targeting this stage are widely disparate [5, 6]. Furthermore, distinguishing elders between normal aging and disease progression type is also an ongoing debate, since elders with normal cognition (NC) may experience SCD as a part of the aging process as well [7]. As it is clear that more thorough characterization and understanding of SCD are required to verify its predictive value for further cognitive decline and to prevent its disease progression, increasing number of researchers have begun focusing on investigating neuroimaging data and biomarkers to identify the underlying mechanisms and values of SCD in predicting disease progression [8, 9].

Daegyeom Kim and Suji Lee contributed equally to this work.

✉ Hyun-Ghang Jeong
jeonghg@korea.ac.kr

✉ Cheol E. Han
cheolhan@korea.ac.kr

[1] Department of Electronics and Information Engineering, Korea University, Sejong, Republic of Korea

[2] Department of Biomedical Sciences, Korea University Graduate School, Seoul, Republic of Korea

[3] Department of Psychiatry, Korea University Guro Hospital, Korea University College of Medicine, Seoul, Republic of Korea

[4] Department of Radiology, Korea University Guro Hospital, Korea University College of Medicine, Seoul, Republic of Korea

It is highly critical to target this stage when the symptoms are subtle yet present. Elderly adults with SCD are more likely to manifest cognitive symptoms that progress to more severe forms of impairment than normal aging elders [10], and such deterioration may affect an individual's daily living [11]. Neuroimaging analyses such as volumetric studies [2, 12] and functional imaging analysis [13] have also highlighted the significant brain changes that are related with disease progression in SCD. For example, Yue et al. stressed the differences between elders with SCD and normal aging elders by proposing that elders with SCD exhibit not only gray matter reduction in the right amygdala and hippocampus but also imbalanced degenerative features in both hemispheres while the normal aging elders do not [14]. Thus, it is of interest to investigate the markers that can be used to detect the differences between elders who are likely to develop the disease and normal aging individuals for early intervention and possible delay of disease progression.

Given that the distinction between SCD and normal aging is essential, earlier findings suggest that defining the architecture of inter-region interactions beyond that of a single area of the brain is highly significant, as reciprocal activation of distributed regions facilitates complex cognitive functions [2, 15, 16]. In this respect, graph theoretical analysis can be a useful instrument to investigate the interactive dynamics of the brain network. Graph theoretical analysis considers the whole brain a network consisting of nodes that correspond to brain regions and edges representing the relationship between any pair of brain regions. This approach has been successful in identifying organizational changes of the brain in patients with various neurological disorders [17, 18]. In this regard, we can postulate that unraveling of the complex inter-region connectivity in the brain may contribute to early detection of the potential progression of SCD to AD. Moreover, since SCD may occur before MCI stage which then has a higher chance of converting to AD [9, 16], investigating the network connectivity profiles associated with SCD may provide a key to understand and predict the disease progression pattern.

Therefore, we aimed to investigate the substrates of alterations in brain networks using diffusion-weighted images (DWI) in elderly adults with SCD to better explain and predict their potential disease progression. We adopted network-based statistics (NBS) to extract abnormal brain subnetworks and localize abnormal brain connectivity. This analysis method [19] offers a powerful and complementary approach towards these objectives and has proven successful in clinical applications [20]. NBS employs family-wise multiple comparison corrections similar to random field theory [21] in voxel-based morphometry. Through this, we sought to determine if the network characteristics of the brain networks in SCD correlates with performance on cognitive tasks.

Materials and methods

Subjects

A total of 44 subjects were recruited from the Korea University Guro Hospital. The subjects included 18 subjects with NC and 26 subjects with SCD. NC subjects were age- and gender-matched (Table 1). The subjects were recruited on a voluntary basis and were provided with appropriate instructions. The NC subjects had no previous history of neurologic or psychiatric illness or current cognitive symptoms. The inclusion criteria of the SCD subjects are individuals who: (1) were 60 years or above, (2) complained about their SCD symptoms before, and (3) scored within the normal range on the neurocognitive battery including word list memory, word list recognition, word list recall, constructional praxis, Boston naming test, verbal fluency, and trail making tests, (> -1.5 standard deviation of the mean established for age-, education-, and sex-matched controls). Individuals with vascular lesions, other neurological disorders (e.g., encephalosclerosis, epilepsy, or traumatic brain injury), cardiac pacemakers which can affect the results of magnetic resonance imaging (MRI), claustrophobia, or substance use disorders were excluded from this study. A neuroradiologist reviewed all the obtained images and ruled out patients with the abovementioned conditions as part of the screening process. All participants underwent a standardized neurocognitive battery called the Consortium to Establish a Registry for Alzheimer's Disease (CERAD) neurocognitive battery and Montreal Cognitive Assessment (MOCA). This study was approved by the Institutional Review Board of Korea University Guro Hospital. Informed consent was obtained from every participant.

Image acquisition

MRI data of all 44 subjects were acquired on a 3.0-Tesla Siemens Trio Trim scanner at Korea University Guro Hospital. For each of the subjects, two sets of DWI were obtained at a single-scan session with a standard single-shot, SE-EPI sequence with eddy current balanced diffusion weighting gradient pulses, where each set of DWI consists a reference volume and 20 volumes with gradient directions. The parameters of this imaging protocol were: $b = 1000$ s/mm^2, TE/TR = 84 ms/6.3 s; matrix = 128 × 128 on 230 × 230 mm FOV; and 3-mm slices without a gap resulting in voxels of 1.8 × 1.8 × 3.0 mm. Adequate signal-to-noise ratios were provided by the average of the four magnitudes. T1-weighted images were acquired using a magnetization-prepared rapid gradient-echo sequence (TE/TR/TI = 2.60 ms/1.9 s/900 ms; 256 × 256 × 176 matrix for 0.86 × 0.86 × 1 mm voxels).

Table 1 We are sorr for the mass. We found that this table is from the old draft. Characteristics of the subjects

Item	NC	SCD	*t* statistics	*p* value
Age	70.61 ± 7.54[1]	69.12 ±8.08	0.62	0.538
Gender (male/female)	8/10	7/19	Yates' $\chi^2 = 0.778$	0.378
Education	10.78 ± 5.58	6.38 ± 5.43	2.56	0.014
APOE (APOE4−/APOE4+)	13/5	17/9	Yates' $\chi^2 = 0.022$	0.882
MMSE	27.06 ± 3.05	24.00 ± 4.38	2.50	0.016
CERAD				
Constructional praxis	9.94 ± 2.01	9.16 ±1.60	1.40	0.170
Word list memory	17.12 ± 5.19	15.60 ± 4.51	1.01	0.320
Word list recall	6.82 ± 1.13	5.32 ± 2.06	2.74	0.009
Word list recognition	9.41 ± 0.71	8.88 ± 1.13	1.72	0.093
Constructional recall	8.12 ± 2.20	5.60 ± 3.06	2.92	0.006
Verbal fluency	15.82 ± 3.99	13.28 ± 3.23	2.28	0.028
Boston naming test	12.94 ± 2.11	10.72 ±2.64	2.90	0.006
MOCA				
Visuoconstructional skill (cube)	0.69 ± 0.48	0.52 ± 0.51	0.98	0.333
Delayed recall	2.00 ± 1.47	0.91 ±1.31	2.29	0.029

[1] Mean ± standard deviation

NC, normal control; *SCD*, subjective cognitive deficits; *MMSE*, mini-mental state examination; *CERAD*, Consortium to Establish a Registry for Alzheimer's Disease; *MOCA*, Montreal Cognitive Assessment

Image preprocessing and network construction

To extract brain networks from MR images, we preprocessed DWI and T1-weighted images. For the DWIs, we merged two sets of diffusion-weighted volumes using the following procedure since the DWI was acquired twice in each subject. We first divided the two sets of DWI. Each of them contained 20 volumes with the gradient directions and 1 reference volume without the gradient direction. We then performed the eddy-current correction of FMRIB's Diffusion Toolbox (v.3.0) separately for the two sets of DWI to remove unwanted movements by registering all volumes with the gradient directions to their own reference volume. Subsequently, by registering reference volumes of the two sets of DWI, we aligned the two sets of the eddy current–corrected DWIs. We appropriately rotated the gradient direction vectors during the alignment procedure described above. Finally, the two reference volumes were averaged, resulting in a single reference volume. All of the preprocessing steps detailed above were performed with the FSL Toolkit (v5.0.9) (https://fsl.fmrib.ox.ac.uk/fsl/fslwiki). To obtain streamline tractography from the processed diffusion-weighted images, we used the Fiber Assignment by Continuous Tracking (FACT) algorithm with 45° of angular threshold through diffusion toolkit along with Trackvis (v0.6.0.1) [22, 23]. To remove artifacts in the tractography, we used a brain mask which only contains the white matter; we used FMRIB's automated segmentation tool (FAST) [24] over each subject's T1-weighted image, and aligned to the diffusion space of the subject using the affine registration method (see the next paragraph for the alignment). FAST segments brain images into different tissue types based on the intensity distribution: gray matter, white matter, and CSF. Thus, all seeds are in the white matter.

We defined the regions of interests (ROIs) using automated anatomical labeling [8, 25] by co-registering the DWI with the T1-weighted image and registering the T1-weighted image with the standard MNI template (http://www.cma.mgh.harvard.edu/fsl_atlas.html). For the T1-weighted images, we first extracted brains by removing nonbrain tissues using a Brain Extraction Tool (v2.1) of the FSL Toolkit. Following this, we nonlinearly registered the brain image with the standard MNI brain template in which the AAL atlas resides using FSL nonlinear registration toolbox (v.6.0). We also performed co-registration between the DWI and T1-weighted images of each subject using the affine registration method (FSL's linear registration toolbox v.6.0, Rigid-body). Then, we transformed the ROIs (i.e., brain regions) defined in the AAL atlas into the diffusion space of each subject by inversely applying the registration parameters. We excluded the ROIs in the cerebellum, since our MRI protocol is not appropriate for tractography and connectome analysis of the cerebellum. Thus, the number of ROIs is 90 (78 cortical and 12 subcortical brain regions).

After preprocessing the DWIs and T1-weighted images, we obtained connectivity matrices from the defined and registered ROIs and tractography by counting the number of tracks between any pair of ROIs using the UCLA multimodal connectivity package (UMCP, http://ccn.ucla.edu/wiki/index.php): the nodes are anatomically defined ROIs and the edge

weights are the number of tracks between any pair of ROIs. As a result, we obtained a 90-by-90 connectivity matrix since we used 90 brain regions as nodes. We excluded the connections which do not exist in at least 50% of subjects of the NC group [26].

Network measures

We computed network measures using the Brain Connectivity Toolbox [27] to quantify the local and global properties of the network. We used the following measures: nodal degree, nodal strength, clustering coefficient, local efficiency, global efficiency, participation coefficient, and regional efficiency. The nodal degree indicates how many neighboring nodes the node is connected with. The nodal strength indicates how strongly the node is connected with its neighboring nodes, by summing all edge weights connected with the node. The clustering coefficient indicates how strongly the node is connected to its neighboring nodes [28]. The local efficiency indicates how well a node exchanges information with its neighboring nodes. The global efficiency is the harmonic mean of shortest path lengths between all pairs of nodes and is related to the information exchanges over the whole network. While the local efficiency indicates the level of local functional segregation, the global efficiency represents the level of global integration of the network. The participation coefficient indicates the importance of a node in the between-module communication where a larger value represents that more information can be exchanged between modules through the node [28, 29]. The regional efficiency indicates how efficiently information of a node can be exchanged to all other nodes.

Statistical analysis

Network-based statistics (NBS) was used to identify subnetworks that are associated with a group difference between NC subjects and SCD subjects, where the subnetwork is a set of connected edges whose statistics exceed a certain threshold value [19, 30]. NBS is a method based on the principles underlying traditional cluster-based thresholding of statistical parametric maps to control family-wise error rate when mass univariate testing is performed at every connection of the graph. The purpose of using NBS in a case-control study is to identify any pairwise associations that are significantly different between groups with an appropriate multiple comparison correction. Specifically, NBS uses permutation testing to evaluate the significance levels of group differences based on how much larger the size of subnetworks is compared with randomly formed subnetworks. We empirically selected the threshold, which provided stable clusters over multiple runs with different permutation vectors and small perturbation of the thresholds. Though the threshold may affect the identified networks, the significance level calculated by the cluster-wise multiple comparison correction is always valid [31]. To control the effects of age, gender, and the duration of education, we used the general linear model (GLM) shown below.

$$w = \beta_0 + \beta_1 \times \text{group} + \beta_2 \times \text{age} + \beta_3 \times \text{gender} + \beta_4 \times \text{education}$$

where w is the edge weights. We used t statistics for the group information; β_1 as a representative statistic for NBS and set a threshold for NBS to 2.5.

Correlation analysis

We then performed correlation analysis between the network measures of identified nodes through NBS and the neurocognitive battery with controlling for the effects of gender, age, and the duration of education in the SCD group following our previous work [32]. Then, p values were adjusted through the false discovery rate (FDR) procedure over the nodes in each of the subnetworks separately [33]. We also performed correlation analysis between edge weights of identified edges through NBS and a neurocognitive battery with controlling for the effects of gender, age, and the duration of education in the SCD group and the FDR procedure over the edges in each of the subnetworks separately. This correlation study may show that the identified nodes and edges have crucial roles in cognitive function.

Visualization

We used in-house Matlab codes to depict a subnetwork over a transparent brain, which show nodes of the AAL90 and significant edges over a transparent cortical mesh surface of the FreeSurfer's average subject [34]. All analysis and visualization were performed using Matlab 8.1 (64bit version, R2013a, Mathworks, Natick, USA).

Results

Subject characteristics

The average age and the gender ratio were not different between the SCD group and the NC group, while the education duration was shorter in the SCD group. Cognitive performance as demonstrated by the mini-mental state examination (MMSE), word list recall, constructional recall, verbal fluency, and Boston naming test was worse in the SCD group than in the NC group (Table 1).

Abnormal subnetwork in SCD

NBS was performed with controlling of the effects of age, gender, and the duration of education, because the duration of education was not matched between the two groups. We used the NBS threshold of 2.5 with 10,000 permutations. We discovered two subnetworks (Fig. 1). Subnetwork 1 contains 4 edges (corrected $p = 0.011$) that connected with 5 nodes including the right putamen, superior parietal, angular, and precentral and postcentral cortices. Subnetwork 2 contains 4 edges (corrected $p = 0.040$) that connect 5 nodes including the left superior medial frontal gyrus, paracentral lobule, the right precuneus, posterior cingulum, and supplementary motor area. All edges had decreased edge weights in SCD subjects (Fig. 2, Table 2). Except the left superior medial frontal gyrus and paracentral lobule, all identified brain regions connected with the subnetworks were in the right hemisphere.

We then performed correlation analysis between the abnormal edges of the identified subnetworks and neurocognitive battery scores of SCD subjects. There was no significant correlation between the weights of the edges identified by NBS and the neurocognitive battery scores.

Association between node characteristics and cognitive decline

We investigated the correlation between network properties of all identified nodes and the neurocognitive battery scores controlling for age, gender, and the level of education (Table 3). We found the significant association only in subnetwork 1; there was no significant correlation results with the connections in subnetwork 2. The used network properties showed various aspects of network centrality. The regional efficiency captures how efficiently information of a brain region can be exchanged to all other brain regions. The regional efficiency was positively correlated with the word list recall score, the right putamen ($r = 0.495$, FDR adjusted $p = 0.027$, unless mentioned, all p values in this paragraph are FDR adjusted), the right superior parietal ($r = 0.589$, $p = 0.016$), and angular gyrus ($r = 0.531$, $p = 0.023$). The nodal strength captures how strongly a brain region is connected with its directly-connected neighboring brain regions; a larger value indicates that a brain region strongly affects its neighboring brain regions. The nodal strength of the right superior parietal is positively correlated with the word list recognition score ($r = 0.548$, $p = 0.034$). The nodal degree of the right postcentral is negatively correlated with Boston naming test score ($r = -0.575$, $p = 0.020$) which captures similar concept with the nodal strength.

Discussion

This study reported the differences in the brain networks between subjects with SCD and NC using DWI. Through NBS analysis, we revealed that the altered subnetworks in SCD include the superior parietal gyrus, angular gyrus, precuneus, posterior cingulum, putamen, precentral gyrus, postcentral gyrus, and paracentral lobule. Furthermore, the results of the correlation analysis indicate that such distinct network alterations found in SCD are correlated with some of the key cognitive domains such as memory and frontal executive functions which are significantly related to those of patients with AD. The results obtained from this present work are consistent with our hypothesis that alterations in the brain network begin in the SCD stage and may be a harbinger of continuous cognitive decline.

Our study reveals altered organization of subnetwork in SCD located in the notable regions that overlap with the affected areas of the brain in MCI and AD. The precuneus and posterior cingulum which participate in a great deal of cognitive functioning such as memory, thought-processing, and visuospatial skills play an essential role in composing the default mode network (DMN) [35]. DMN, the state of neural connectivity while the brain is at rest, often exhibits weaker interconnections among the regions such as the precuneus, posterior cingulum, and hippocampus throughout the disease progression [36]. In addition, these specific regions are particularly susceptible to accumulation of amyloid beta protein which is one of the hallmarks of AD pathology, and such aberrant activity in their connectivity contribute to the failure of memory formation and retrieval [37]. Likewise, another study using the resting-state functional MRI and graph theory found an unlikely state of network involving the putamen in patients with amnestic MCI (aMCI) which is considered as the prodromal phase of AD [38]. The putamen, located in the subcortex of the brain, is part of the striatum responsible for cortico-thalamic projections [39]. When compared with those of NC group, the putamen and superior medial frontal gyrus of AD population constituted less optimal functional connectivity [40]. We speculate that the impairment in the abovementioned intrinsic connectivity may cause inefficient transfer of information and manifest deficits in cognitive functioning in SCD.

Some brain regions found in this study, on the other hand, namely the postcentral gyrus, precentral gyrus, and supplementary motor area, have been less commonly identified as pronounced regions associated with AD in SCD. According to the preceding findings, these regions do not appear to be impaired in the beginning stage of AD or beforehand [41]; however, several evidences drawn by functional neuroimaging techniques support their later relationship with AD pathology. For example, Huang et al. recently investigated metabolic connectivity using the fluorodeoxyglucose-positron emission tomography (FDG-PET) and found a lowered number of

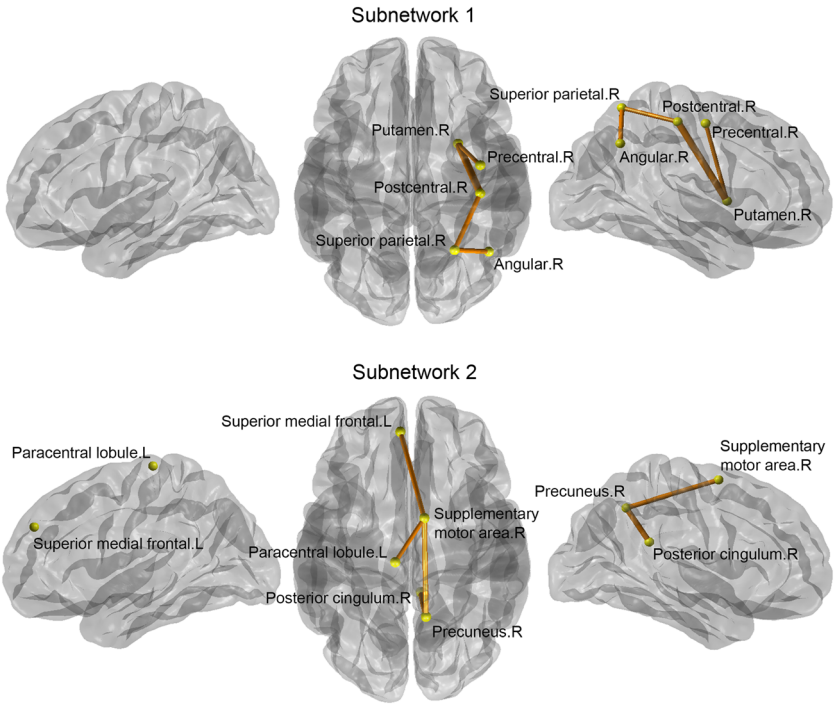

Fig. 1 The identified subnetwork by NBS. The subnetwork was identified using network-based statistics (NBS) with a threshold value of 2.5 and 10,000 permutations. The left column shows the lateral view of the left hemisphere, the middle column shows the transverse view of the both hemispheres, and the right column shows the lateral view of the right hemisphere. The yellow circles are brain regions while the orange lines are edges where their thickness represents the strength of the connectivity differences (*t* statistics). All edges decreased in subjective cognitive deficits (SCD) subjects

functional connectivity in the center of the precentral gyrus and supplementary motor area in patients with AD [42]. Furthermore, a longitudinal single-photon emission computed tomography (SPECT) study demonstrated low cerebral blood flow in the right postcentral gyrus of MCI elders who developed AD within 4 years after the enrollment in the study [43]. Interestingly enough, all these listed regions above were also associated with significant gray matter volume reduction in patients with depressive AD [44]. These findings carefully suggest that identification of the white matter disturbances through NBS analysis using DWI may determine subtle alterations in certain areas of the brain earlier than other modalities such as cerebral metabolism on FDG-PET scans, the brain hypoperfusion on SPECT scans, or cerebral volume on MRI T1 images. Thus, we believe that the disrupted network observed using NBS may be helpful to sort out these subjects at risks from elders with NC in the preclinical stage.

To further investigate the association between the impaired network and cognitive performance in SCD, we conducted a correlation analysis and discovered that the

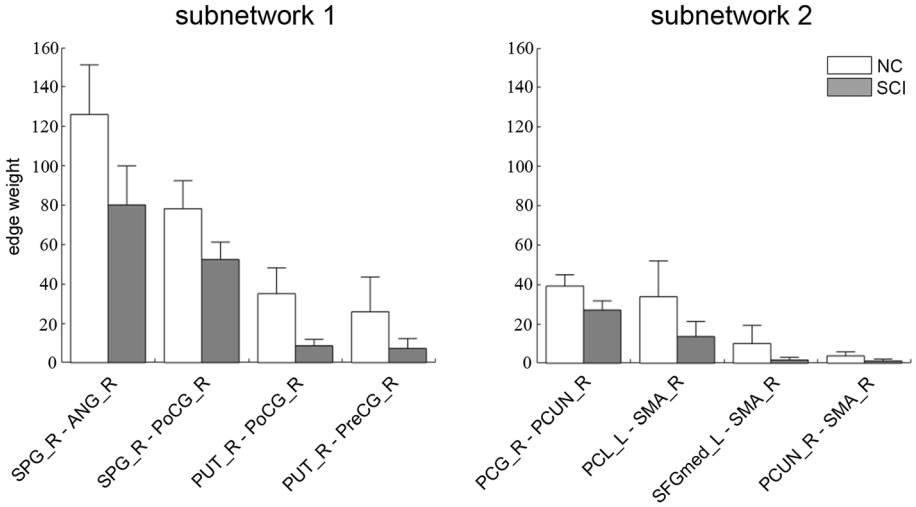

Fig. 2 The average edge weights of connections in the identified subnetworks. The white bars represent the average edge weights of the identified edges in normal controls (NC) and the gray bars represent the edge weights in subjective cognitive deficits (SCD) subjects, with whiskers indicating the 95% confidence intervals. SPG, superior parietal gyrus; ANG, angular gyrus; PoCG, postcentral gyrus; preCG, precentral gyrus; PUT, putamen; PCG, posterior cingulum; PCUN, precunues; PCL, paracentral lobule; SMA, supplementary motor area; SFGmed, superior medial frontal gyrus. L denotes the left hemisphere, and R denotes the right hemisphere

Table 2 Subnetwork identified by network-based statistics (NBS)

Index	Connection	NC	SCD	*t* statistics[1]	*F* statistics[2]
Subnetwork 1	SPG_R–ANG_R	126.11 ± 54.24[3]	80.12 ± 51.55	2.92	8.55 ($p = 0.0057$)
	SPG_R–PoCG_R	78.17 ± 30.82	52.54 ± 22.38	2.84	8.05 ($p = 0.0072$)
	PUT_R–PoCG_R	35.11 ± 28.44	8.62 ± 8.32	4.31	18.56 ($p = 0.0001$)
	PUT_R–PreCG_R	25.89 ± 38.19	7.27 ± 12.99	2.61	6.82 ($p = 0.0127$)
Subnetwork 2	PCG_R–PCUN_R	39.22 ± 5.81	27.08 ± 4.62	3.53	12.48 ($p = 0.0011$)
	PCL_L–SMA_R	33.83 ± 18.23	13.57 ± 7.62	2.51	6.29 ($p = 0.0164$)
	SFGmed_L–SMA_R	10.00 ± 9.26	1.65 ± 1.30	2.84	8.04 (p = 0.0072)
	PCUN_R–SMA_R	3.72 ± 2.08	1.12 ± 1.00	3.11	9.66 ($p = 0.0035$)

[1] *t* statistics of the group difference for the edges identified by NBS. Positive *t* values represent decreased connectivity in the subjective cognitive deficits (SCD) group compared with the normal control group

[2] *F* statistics and the corresponding *p* values using the general linear model controlling for age, gender, and education duration. We used the linstats 2006b toolbox for the *F* statistics and *p* values

[3] Mean ± standard deviation

NC, normal control; *SPG*, superior parietal gyrus; *ANG*, angular gyrus; *PoCG*, postcentral gyrus; *preCG*, precentral gyrus; *PUT*, putamen; *PCG*, posterior cingulum; *PCUN*, precuneus; *PCL*, paracentral lobule; *SMA*, supplementary motor area; *SFGmed*: superior medial frontal gyrus

declining appearances resemble those of AD. First, lower regional efficiency of the putamen was significantly related with the word list recall score which indicates episodic memory, one of the key signs to detect AD in its earlier stage [37]. The putamen, which regulates motor, emotion, motivation, language, and memory [45], plays a pivotal role in the cortico-thalamic circuit by providing the neuronal transference pathway [39]. Given that the regional efficiency, which is defined by how efficiently information can be exchanged to the connected nodes, [46] is found to be low in SCD; it can be inferred that the deterioration of the connectivity in the putamen may cause malfunctioning of the afferent projections of memory information to the cortex. Another region we found correlated with this impaired network measurement and cognitive functioning is the angular gyrus. The angular gyrus is engaged with a broad spectrum of cognitive processes such as calculation, DMN, memory, attention, reasoning, and integration of various inputs [47]. With regard to its relationship with episodic memory, it recollects and converges the information from the previous experiences [48]. The decline of episodic memory function is also often noted in patients with aMCI [49]. Therefore, it may be plausible to suggest that the alteration in the angular gyrus as well implies the beginning of the disease progression in SCD.

Additionally, the superior parietal lobule was found to be associated with weaker nodal strength and lower regional efficiency in SCD group when compared with NC group. This region is known to contribute to visuospatial function and memory [50, 51]. In our study, it displayed weaker strength and reduced efficiency of information transfer when the elders with SCD were working on the word list recall and recognition tests. Evidence supports this correlation between the nodal alterations in the superior parietal lobule and related cognitive dysfunctions in AD as well [52]. Taken together, this may be indicative of the disorganized informational exchange beginning in the early stage of dementia. Last but not least, we discovered a negative correlation between the Boston naming test score and the nodal degree, which refers to the number of connected nodes to its neighboring network [27], in the postcentral gyrus in elders with SCD. The impaired capacity of this language domain may initiate as difficulties in semantic process and eventually affect the perceptual concepts over the course of AD progression [53]. The somatosensory cortex,

Table 3 Correlation between network properties of nodes and clinical measures

Index	Score	Node (network measure)	Correlation[1]
Subnetwork 1	Word list recall	Right putamen (regional efficiency)	$r = 0.495$, $p = 0.027$
		Right superior parietal (regional efficiency)	$r = 0.589$, $p = 0.016$
		Right angular (regional efficiency)	$r = 0.531$, $p = 0.023$
	Word list recognition	Right superior parietal (nodal strength)	$r = 0.548$, $p = 0.034$
	Boston naming	Right postcentral (nodal degree)	$r = -0.575$, $p = 0.020$

[1] Partial correlation coefficient controlling for age, gender, and the level of education after the FDR procedure. The collected *p* values are FDR-adjusted *p* values

which involves the postcentral gyrus, is accountable for semantic analysis of information [54], and the disturbances found in this area of SCD may be due to a fewer local connections and less efficient communication with the nodes in the neighbor zone. Our data thus suggest that the reduced neural collaboration of the postcentral gyrus possibly acts as a potential cause of cognitive decline in SCD.

In our results, most of the detected network alterations were on the right side of the brain. This disproportionate functional segregation between the two hemispheres might be attributed to the imbalanced hemispheric functioning in SCD. A review study summarized that patients with AD exhibit a retained interaction within one hemisphere in contrast to decreased bilateral cooperation during a task [55]. In addition, Vecchio et al. noted that there is a correlation between the aberrant brain network properties and architectural alterations in the right hemisphere of AD patients [56]. Our findings suggest that the imbalance in hemispheric operation may begin as early as in the SCD stage and contribute to interruptions in the integrated brain networks.

This study has some clinical implications. Alterations of brain networks possibly serve as informative markers of the early stage of dementia syndromes. According to DWI analysis of MCI and patients with AD by Huang et al., axonal damage in regions that subserve higher cognitive function, such as the frontal, temporal, and parietal lobes, was detected by Wallerian degeneration [57]. With regard to identifying the at-risks subjects in the precedent stage of AD, it may be possible to detect abnormal brain networks using DWI which may illustrate the subtler cognitive impairment present in SCD. Lopez et al. reported that similar distributions of network disruption were discovered in SCD when compared with a mild form of MCI [5]. Selnes et al. also demonstrated less severe white matter impairment in SCD than in MCI [58]. Therefore, taking these aspects and characteristics of the SCD stage into account may increase the accuracy of predictions of future dementia in the preclinical stage.

Our study unravels the complex subnetworks distinguishing elderly adults with SCD from those with normal cognitive function. Our results provide clearer information on the brain networks that characterize SCD which have potential applications as improved biomarkers of the prodromal phase of dementia. Despite the strengths of the study, there are some limitations that should be considered. First, our study included a small number of subjects resulting in low statistical power. Second, further longitudinal observations might be helpful to confirm the results from our cross-sectional study. Third, our diffusion MRI protocol was suboptimal for tractography. The voxel dimensions were anisotropic ($1.79 \times 1.79 \times 3$ mm), and thus the tractography resulted in a longer z-direction that may affect the overall quality of the tractography. Additionally, the number of gradient directions was rather low (20 directions); however, by recording twice, we overcame much of this shortcoming. Fourth, the inherent limitations of DTI and the deterministic tractography, including the issue of crossing fibers, apply to this study. Other tracking methods, such as probabilistic tractography [59] or Hough Transform global tractography [60], could be employed in future research. Lastly, we did not investigate the complete spectrum of Alzheimer pathology; instead we only compared the brain network between NC and SCD, since our main research aim of this study is investigating the changes in the early stage of dementia.

Conclusion

In summary, we present evidence of alterations in the brain networks in elderly individuals with SCD by using DWI and network analysis. Our results reveal that the alterations in brain networks begin to occur early in the SCD stage. Furthermore, based on our results on SCD and implications from other investigations on MCI and AD, it is plausible to speculate that the disrupted connectivity in SCD may predict disease progression to AD. We also conclude that NBS analysis is a useful approach to detect subtle differences between normal aging elderly adults and those who are in the early stage of dementia-associated disease.

Author contributions HG. Jeong and CE. Han designed the study and supervised the data collection, data analysis, and writing. S. Lee and H. Youn collected the neuroimaging and neurocognitive data and wrote the article. D. Kim and M. Choi carried out the data analysis and wrote the article. Lastly, S. Suh was responsible for data acquisition, subject selection, and quality controls.

Funding information This work was supported by the Korea Health Technology R&D Project through the Korea Health Industry Development Institute (KHIDI) that was funded by the Ministry of Health & Welfare, Republic of Korea (HG.J., HC15C1509, HG.J and CE.H., HI19C0645); the Basic Science Research Program through the National Research Foundation of Korea (NRF), funded by the Ministry of Science and ICT (HG.J., NRF-2015R1C1A1A01052172); and the Basic Science Research Program through the National Research Foundation of Korea (NRF) funded by the Ministry of Education of the Government of the Republic of Korea (CE.H., 2016R1D1A1B03934990).

Compliance with ethical standards

Statement of ethics All human and animal studies have been approved by the appropriate ethics committee and have therefore been performed in accordance with the ethical standards laid down in the 1964 Declaration of Helsinki and its later amendments.

Conflict of interest The authors declare that they have no conflict of interest.

References

1. Rodda J, Dannhauser T, Cutinha DJ, Shergill SS, Walker Z (2011) Subjective cognitive impairment: functional MRI during a divided attention task. Eur Psychiatry 26(7):457–462. https://doi.org/10.1016/j.eurpsy.2010.07.003
2. Hafkemeijer A, Altmann-Schneider I, Oleksik AM, van de Wiel L, Middelkoop HA, van Buchem MA, van der Grond J, Rombouts SA (2013) Increased functional connectivity and brain atrophy in elderly with subjective memory complaints. Brain Connect 3(4):353–362. https://doi.org/10.1089/brain.2013.0144
3. Striepens N, Scheef L, Wind A, Popp J, Spottke A, Cooper-Mahkorn D, Suliman H, Wagner M, Schild HH, Jessen F (2010) Volume loss of the medial temporal lobe structures in subjective memory impairment. Dement Geriatr Cogn Disord 29(1):75–81. https://doi.org/10.1159/000264630
4. Braak H, Braak E (1997) Frequency of stages of Alzheimer-related lesions in different age categories. Neurobiol Aging 18(4):351–357
5. Lopez-Sanz D, Garces P, Alvarez B, Delgado-Losada ML, Lopez-Higes R, Maestu F (2017) Network disruption in the preclinical stages of Alzheimer's disease: from subjective cognitive decline to mild cognitive impairment. Int J Neural Syst 27:1750041. https://doi.org/10.1142/s0129065717500411:1750041
6. Jessen F, Amariglio RE, van Boxtel M, Breteler M, Ceccaldi M, Chetelat G, Dubois B, Dufouil C, Ellis KA, van der Flier WM et al (2014) A conceptual framework for research on subjective cognitive decline in preclinical Alzheimer's disease. Alzheimers Dement 10(6):844–852. https://doi.org/10.1016/j.jalz.2014.01.001
7. Slavin MJ, Brodaty H, Kochan NA, Crawford JD, Trollor JN, Draper B, Sachdev PS (2010) Prevalence and predictors of "subjective cognitive complaints" in the Sydney Memory and Ageing Study. Am J Geriatr Psychiatry 18(8):701–710
8. van der Flier WM, van Buchem MA, Weverling-Rijnsburger AW, Mutsaers ER, Bollen EL, Admiraal-Behloul F, Westendorp RG, Middelkoop HA (2004) Memory complaints in patients with normal cognition are associated with smaller hippocampal volumes. J Neurol 251(6):671–675. https://doi.org/10.1007/s00415-004-0390-7
9. Striepens N, Scheef L, Wind A, Meiberth D, Popp J, Spottke A, Kolsch H, Wagner M, Jessen F (2011) Interaction effects of subjective memory impairment and ApoE4 genotype on episodic memory and hippocampal volume. Psychol Med 41(9):1997–2006. https://doi.org/10.1017/s0033291711000067
10. Jessen F (2014) Subjective and objective cognitive decline at the pre-dementia stage of Alzheimer's disease. Eur Arch Psychiatry Clin Neurosci 264(Suppl 1):S3–S7. https://doi.org/10.1007/s00406-014-0539-z
11. Jenkins A, Tales A, Tree J, Bayer A (2015) Are we ready? The construct of subjective cognitive impairment and its utilization in clinical practice: a preliminary UK-based service evaluation. J Alzheimers Dis 48(Suppl 1):S25–S31. https://doi.org/10.3233/jad-150541
12. Jessen F, Feyen L, Freymann K, Tepest R, Maier W, Heun R, Schild HH, Scheef L (2006) Volume reduction of the entorhinal cortex in subjective memory impairment. Neurobiol Aging 27(12):1751–1756. https://doi.org/10.1016/j.neurobiolaging.2005.10.010
13. Erk S, Spottke A, Meisen A, Wagner M, Walter H, Jessen F (2011) Evidence of neuronal compensation during episodic memory in subjective memory impairment. Arch Gen Psychiatry 68(8):845–852. https://doi.org/10.1001/archgenpsychiatry.2011.80
14. Yue L, Wang T, Wang J, Li G, Wang J, Li X, Li W, Hu M, Xiao S (2018) Asymmetry of Hippocampus and amygdala defect in subjective cognitive decline among the community dwelling Chinese. Front Psychiatry 9:226. https://doi.org/10.3389/fpsyt.2018.00226
15. Shu N, Wang X, Bi Q, Zhao T, Han Y (2018) Disrupted topologic efficiency of white matter structural connectome in individuals with subjective cognitive decline. Radiology 286(1):229–238. https://doi.org/10.1148/radiol.2017162696
16. Wang XN, Zeng Y, Chen GQ, Zhang YH, Li XY, Hao XY, Yu Y, Zhang M, Sheng C, Li YX, Sun Y, Li HY, Song Y, Li KC, Yan TY, Tang XY, Han Y (2016) Abnormal organization of white matter networks in patients with subjective cognitive decline and mild cognitive impairment. Oncotarget 7(31):48953–48962. https://doi.org/10.18632/oncotarget.10601
17. Bullmore E, Sporns O (2009) Complex brain networks: graph theoretical analysis of structural and functional systems. Nat Rev Neurosci 10(3):186–198. https://doi.org/10.1038/nrn2575
18. Sporns O (2010) Networks of the brain. MIT Press, Cambridge
19. Zalesky A, Fornito A, Bullmore ET (2010) Network-based statistic: identifying differences in brain networks. Neuroimage 53(4):1197–1207. https://doi.org/10.1016/j.neuroimage.2010.06.041
20. Filippi M, Basaia S, Canu E, Imperiale F, Meani A, Caso F, Magnani G, Falautano M, Comi G, Falini A, Agosta F (2017) Brain network connectivity differs in early-onset neurodegenerative dementia. Neurology 89(17):1764–1772. https://doi.org/10.1212/wnl.0000000000004577
21. Worsley KJ, Evans AC, Marrett S, Neelin P (1992) A three-dimensional statistical analysis for CBF activation studies in human brain. J Cereb Blood Flow Metab 12(6):900–918. https://doi.org/10.1038/jcbfm.1992.127
22. Mori S, Barker PB (1999) Diffusion magnetic resonance imaging: its principle and applications. Anat Rec 257(3):102–109
23. Wang R, Benner T, Sorensen A, Wedeen VJ (2007) Diffusion toolkit: a software package for diffusion imaging data processing and tractography. Proc Intl Soc Mag Reson Med 15:3720
24. Zhang Y, Brady M, Smith S (2001) Segmentation of brain MR images through a hidden Markov random field model and the expectation-maximization algorithm. IEEE Trans Med Imaging 20(1):45–57. https://doi.org/10.1109/42.906424
25. Tzourio-Mazoyer N, Landeau B, Papathanassiou D, Crivello F, Etard O, Delcroix N, Mazoyer B, Joliot M (2002) Automated anatomical labeling of activations in SPM using a macroscopic anatomical parcellation of the MNI MRI single-subject brain. Neuroimage 15(1):273–289. https://doi.org/10.1006/nimg.2001.0978
26. de Reus MA, van den Heuvel MP (2013) Estimating false positives and negatives in brain networks. Neuroimage 70:402–409. https://doi.org/10.1016/j.neuroimage.2012.12.066
27. Rubinov M, Sporns O (2010) Complex network measures of brain connectivity: uses and interpretations. Neuroimage 52(3):1059–1069. https://doi.org/10.1016/j.neuroimage.2009.10.003
28. Watts DJ, Strogatz SH (1998) Collective dynamics of 'small-world' networks. Nature 393(6684):440–442. https://doi.org/10.1038/30918
29. Guimerà R, Nunes Amaral LA (2005) Functional cartography of complex metabolic networks. Nature 433(7028):895–900. https://doi.org/10.1038/nature03288
30. Zalesky A, Fornito A, Seal ML, Cocchi L, Westin CF, Bullmore ET, Egan GF, Pantelis C (2011) Disrupted axonal fiber connectivity in schizophrenia. Biol Psychiatry 69(1):80–89. https://doi.org/10.1016/j.biopsych.2010.08.022
31. Smith SM, Jenkinson M, Johansen-Berg H, Rueckert D, Nichols TE, Mackay CE, Watkins KE, Ciccarelli O, Cader MZ, Matthews PM, Behrens TEJ (2006) Tract-based spatial statistics: voxelwise analysis of multi-subject diffusion data. Neuroimage 31(4):1487–1505. https://doi.org/10.1016/j.neuroimage.2006.02.024
32. Myung W, Han CE, Fava M, Mischoulon D, Papakostas GI, Heo JY, Kim KW, Kim ST, Kim DJ, Kim DK et al (2016) Reduced frontal-subcortical white matter connectivity in association with suicidal ideation in major depressive disorder. Transl Psychiatry 6(6):e835. https://doi.org/10.1038/tp.2016.110

33. Benjamini Y, Hochberg Y (1995) Controlling the false discovery rate: a practical and powerful approach to multiple testing. J R Stat Soc Ser B Stat Methodol 57(1):289–300
34. Fischl B, Dale AM (2000) Measuring the thickness of the human cerebral cortex from magnetic resonance images. Proc Natl Acad Sci U S A 97(20):11050–11055. https://doi.org/10.1073/pnas.200033797
35. Greicius MD, Srivastava G, Reiss AL, Menon V (2004) Default-mode network activity distinguishes Alzheimer's disease from healthy aging: evidence from functional MRI. Proc Natl Acad Sci U S A 101:4637–4642. https://doi.org/10.1073/pnas.0308627101
36. Wang Y, Risacher SL, West JD, McDonald BC, Magee TR, Farlow MR, Gao S, O'Neill DP, Saykin AJ (2014) Altered default mode network connectivity in older adults with cognitive complaints and amnestic mild cognitive impairment. J Alzheimers Dis 35:751–760. https://doi.org/10.3233/jad-130080
37. Sperling RA, Laviolette PS, O'Keefe K, O'Brien J, Rentz DM, Pihlajamaki M, Marshall G, Hyman BT, Selkoe DJ, Hedden T et al (2010) Amyloid deposition is associated with impaired default network function in older persons without dementia. Neuron. 63:178–188. https://doi.org/10.1016/j.neuron.2009.07.003
38. Wang J, Zuo X, Dai Z, Xia M, Zhao Z, Zhao X, Jia J, Han Y, He Y (2013) Disrupted functional brain connectome in individuals at risk for Alzheimer's disease. Biol Psychiatry 73:472–481. https://doi.org/10.1016/j.biopsych.2012.03.026
39. de Jong LW, van der Hiele K, Veer IM, Houwing JJ, Westendorp RGJ, Bollen ELEM, de Bruin PW, Middelkoop HAM, van Buchem MA, van der Grond J (2008) Strongly reduced volumes of putamen and thalamus in Alzheimer's disease: an MRI study. Brain. 131:3277–3285. https://doi.org/10.1093/brain/awn278
40. Yao H, Liu Y, Zhou B, Zhang Z, An N, Wang P, Wang L, Zhang X, Jiang T (2013) Decreased functional connectivity of the amygdala in Alzheimer's disease revealed by resting-state fMRI. Eur J Radiol 82:1531–1538. https://doi.org/10.1016/j.ejrad.2013.03.019
41. Braak H, Braak E (1991) Neuropathological stageing of Alzheimer-related changes. Acta Neuropathol 82(4):239–259
42. Huang S-Y, Hsu J-L, Lin K-J, Liu H-L, Wey S-P, Hsiao I-T, Alzheimer's Disease Neuroimaging I (2018) Characteristic patterns of inter- and intra-hemispheric metabolic connectivity in patients with stable and progressive mild cognitive impairment and Alzheimer's disease. SC Reports. https://doi.org/10.1038/s41598-018-31794-8
43. Alegret M, Cuberas-Borros G, Espinosa A, Valero S, Hernandez I, Ruiz A, Becker JT, Rosende-Roca M, Mauleon A, Sotolongo O et al (2014) Cognitive, genetic, and brain perfusion factors associated with four year incidence of Alzheimer's disease from mild cognitive impairment. J Alzheimers Dis 41(3):739–748. https://doi.org/10.3233/jad-132516
44. Karavasilis E, Parthimos TP, Papatriantafyllou JD, Papageorgiou SG, Kapsas G, Papanicolaou AC, Seimenis I (2017) A specific pattern of gray matter atrophy in Alzheimer's disease with depression. https://doi.org/10.1007/s00415-017-8603-z
45. Leto L, Feola M (2014) Cognitive impairment in heart failure patients. J Geriatr Cardiol 11(4):316–328. https://doi.org/10.11909/j.issn.1671-5411.2014.04.007
46. Achard SBE (2007) Efficiency and cost of economical brain functional networks. PLoS Comput Biol 3:e17
47. Seghier ML (2012) The angular gyrus: multiple functions and multiple subdivisions. Neuroscientist 19:43–61. https://doi.org/10.1177/1073858412440596
48. Bonnici HM, Richter FR, Yazar Y, Simons JS (2016) Multimodal feature integration in the angular gyrus during episodic and semantic retrieval. J Neurosci 36:5462–5471. https://doi.org/10.1523/jneurosci.4310-15.2016
49. Xie C, Bai F, Yu H, Shi Y, Yuan Y, Chen G, Li W, Chen G, Zhang Z, Li S-J (2015) Abnormal insula functional network is associated with episodic memory decline in amnestic mild cognitive impairment. Neuroimage. 63:320–327. https://doi.org/10.1016/j.neuroimage.2012.06.062
50. Jacobs HI, Van Boxtel MP, Jolles J, Verhey FR, Uylings HB (2012) Parietal cortex matters in Alzheimer's disease: an overview of structural, functional and metabolic findings. Neurosci Biobehav Rev 36(1):297–309. https://doi.org/10.1016/j.neubiorev.2011.06.009
51. Koenigs M, Barbey AK, Postle BR, Grafman J (2009) Superior parietal cortex is critical for the manipulation of information in working memory. J Neurosci 29(47):14980–14986. https://doi.org/10.1523/jneurosci.3706-09.2009
52. Ng VW, Bullmore ET, de Zubicaray GI, Cooper A, Suckling J, Williams SC (2001) Identifying rate-limiting nodes in large-scale cortical networks for visuospatial processing: an illustration using fMRI. J Cogn Neurosci 13(4):537–545
53. Hodges JR, Salmon DP, Butters N (1991) The nature of the naming deficit in Alzheimer's and Huntington's disease. Brain. 114:1547–1558. https://doi.org/10.1093/brain/114.4.1547
54. Flanagan KJ, Copland DA, Chenery HJ, Byrne GJ, Angwin AJ (2013) Alzheimer's disease is associated with distinctive semantic feature loss. Neuropsychologia. 51:2016–2025. https://doi.org/10.1016/j.neuropsychologia.2013.06.008
55. Delbeuck X, Van der Linden M, Collette F (2003) Alzheimer's disease as a disconnection syndrome. Neuropsychol Rev 13(2):79–92
56. Vecchio F, Miraglia F, Piludu F, Granata G, Romanello R, Caulo M, Onofrj V, Bramanti P, Colosimo C, Rossini PM (2017) "Small world" architecture in brain connectivity and hippocampal volume in Alzheimer's disease: a study via graph theory from EEG data. Brain Imaging Behav 11(2):473–485. https://doi.org/10.1007/s11682-016-9528-3
57. Huang J, Friedland RP, Auchus AP (2007) Diffusion tensor imaging of normal-appearing white matter in mild cognitive impairment and early Alzheimer disease: preliminary evidence of axonal degeneration in the temporal lobe. AJNR Am J Neuroradiol 28(10):1943–1948. https://doi.org/10.3174/ajnr.A0700
58. Selnes P, Fjell AM, Gjerstad L, Bjornerud A, Wallin A, Due-Tonnessen P, Grambaite R, Stenset V, Fladby T (2012) White matter imaging changes in subjective and mild cognitive impairment. Alzheimers Dement 8(5 Suppl):S112–S121. https://doi.org/10.1016/j.jalz.2011.07.001
59. Behrens TE, Berg HJ, Jbabdi S, Rushworth MF, Woolrich MW (2007) Probabilistic diffusion tractography with multiple fibre orientations: what can we gain? Neuroimage 34(1):144–155. https://doi.org/10.1016/j.neuroimage.2006.09.018
60. Aganj I, Lenglet C, Jahanshad N, Yacoub E, Harel N, Thompson PM, Sapiro G (2011) A Hough transform global probabilistic approach to multiple-subject diffusion MRI tractography. Med Image Anal 15(4):414–425. https://doi.org/10.1016/j.media.2011.01.003